Journal of Molecular Catalysis B: Enzymatic 83 (2012) 38–45

Contents lists available at SciVerse ScienceDirect

Journal of Molecular Catalysis B: Enzymatic

journal homepage: www.elsevier.com/locate/molcatb

Enzymatic kinetic resolution of hydroxystearic acids: A combined experimental and molecular modelling investigation

Cynthia Ebert[a], Fulvia Felluga[a], Cristina Forzato[a], Marco Foscato[a], Lucia Gardossi[a], Patrizia Nitti[a,*], Giuliana Pitacco[a], Carla Boga[b,**], Paolo Caruana[b], Gabriele Micheletti[b], Natalia Calonghi[c], Lanfranco Masotti[c]

[a] Dipartimento di Scienze Chimiche e Farmaceutiche, Università di Trieste, via Licio Giorgieri 1, I-34127 Trieste, Italy
[b] Dipartimento di Chimica Organica 'A. Mangini' Alma Mater Studiorum, Università di Bologna Viale Risorgimento, 4-40136 Bologna, Italy
[c] Dipartimento di Biochimica 'G. Moruzzi' Alma Mater Studiorum, Università di Bologna Via Irnerio, 48-40126 Bologna, Italy

ARTICLE INFO

Article history:
Received 17 May 2012
Received in revised form 28 June 2012
Accepted 30 June 2012
Available online 10 July 2012

Keywords:
Hydroxystearic acids
Enzymatic resolution
CALB
Molecular recognition
Enantioselectivity

ABSTRACT

Enantioenriched 7-, 8-, 9-, and 10-hydroxystearic acids (HSA) were obtained, for the first time, by kinetic resolution of their racemates with lipases CALB and PS, in the presence of vinyl acetate. Among them, the best results were obtained for 7-HSA and 9-HSA, whose enantiomeric excess was around 55%. The same resolutions carried out on the hydroxy esters completely failed. For the acid substrates neither the Kazlauskas' rule nor the 3D-QSAR model could be applied, since both models are focused on the CALB alcohol-pocket evaluation and not on the acyl-pocket one. Therefore, a semiquantitative approach was used, whose results were in accordance with our findings, as far as the absolute configuration of the product is concerned.

1. Introduction

Hydroxy fatty acids and their derivatives belong to a class of compounds of growing interest in many areas. Apart from being essential molecules in many biological processes [1,2], they are also used in a variety of industrial processes [3–10] and more recently also in material chemistry [11].

In connection with their biological activities, the most studied members of the series have been 9- and 10-hydroxystearic acids (9- and 10-HSA), for their natural negative regulatory activity of tumour cell proliferation [12]. Recently [13], 9-HSA has been found to play an important role in cancerogenesis of HT29, a human colon adenocarcinoma cell line, acting as a competitive inhibitor of HDAC1 (histone deacetylase 1) isoform [14]. Furthermore, studies of molecular docking [14] have shown a more favourable binding energy for the HDAC1-(*R*)-9-HSA complex, as compared to the (*S*) complex. Therefore the availability of hydroxystearic acids in enantiopure forms seems an attractive challenge.

In general, their natural precursors are unsaturated hydroxy fatty acids contained in seeds of higher plants [15]. For example, oleic acid can be converted into 10-HSA with a variety of bacterial species or yeasts [16], (*S*)-dimorphecolic acid present in large amount in the seeds of genus Dimorphotheca, can be a precursor of (*R*)-9-HSA [15] while D-ricinoleic acid, obtained from castor oil, can be a precursor of (*R*)-12-HSA [17]. Less available from natural sources are precursors of 8-HSA, namely isanolic acid [15,18] and laetisaric acid [19], whereas no useful natural precursor of 7-HSA is known. Obviously, since the choice of the plant must take into account both its availability and the relative amount of the desired compound in the seed oil, an enantioselective synthesis might be envisaged as a preferable route.

Enantioselective chemical syntheses of hydroxystearic acids or their unsaturated precursors have been reported only in a few cases [20] and require multi-step synthetic strategies. On the other hand, it is well-known how difficult it is to achieve a high degree of enantioselectivity in the reduction of carbonyl compounds with a *quasi* symmetric long-chain substitution [21]. The same difficulties were encountered for biocatalysed reductions that gave good results only for short-chain γ- and δ-ketoacids [22,23].

All these results prompted us to investigate the possibility of preparing a few members of the series in optically pure form, by the use of enzymes. The scope was also to explore how the stereochemical course could depend on the position of the hydroxyl group along the chain, especially when situated far from the terminus of the chain. In this preliminary study, Lipase B from *Candida*

* Corresponding author. Tel.: +39 0 405583923; fax: +39 0 405583903.
** Corresponding author. Tel.: +39 0 512093616.
E-mail addresses: pnitti@units.it (P. Nitti), carla.boga@unibo.it (C. Boga).

1381-1177/$ – see front matter © 2012 Elsevier B.V. All rights reserved.
http://dx.doi.org/10.1016/j.molcatb.2012.06.017

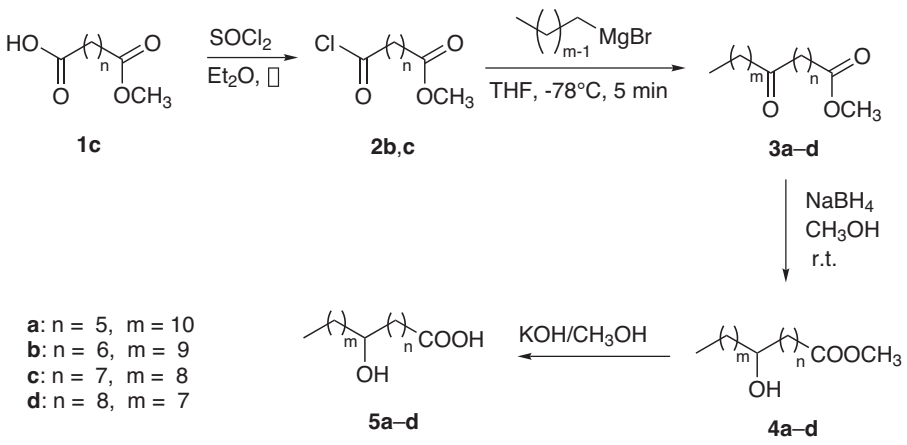

Scheme 1. Synthesis of isomeric HSAs **5a–d**.

antarctica (CALB) and lipase from *Pseudomonas cepacia* were chosen since the experimental outcomes could be compared with theoretical studies. In fact, the resolution of racemic compounds by CALB is one of the most studied biocatalytic systems [24]. In hydrolysis/synthesis of esters, the enantiopreference is predicted by Kazlauskas' rule [25] that assesses that in the case of a secondary alcohol with two substituents of different steric encumbrance the (*R*)-enantiomer reacts preferentially. This was confirmed by molecular modelling studies [24–28] and, more recently, by three-dimensional structure-activity models (3D-QSAR) [29a,29b]. Being aware of the challenge represented by the resolution of these particular bulky and *quasi* symmetric secondary alcohols, a preliminary computational analysis was performed. Docking, molecular dynamic simulations and 3D-QSAR models were used to verify the ability of the enzyme to recognize and transform these substrates. A comparison was also made with the lipase from *P. cepacia*. The results emerged from the computational analysis were also supported by the experimental data, which confirmed how the secondary hydroxyl group on the fatty acid chain is in an unfavourable position both in terms of reactivity and in terms of enzyme enantiodiscrimination.

2. Results and discussion

Racemic 7-, 8-, 9-, and 10-hydroxystearic acids (HSA) **5a–d** were synthesized by chemical reduction of the corresponding 7-, 8-, 9-, and 10-ketoesters **3a–d** (Scheme 1), followed by hydrolysis under basic conditions [12c,30]. Compounds **3a** and **3d** are commercially available while **3b** and **3c** were prepared from **2b** (commercially available) and **2c**, respectively, by addition of the appropriate Grignard reagent. Compound **2c** was in turn prepared from azelaic acid monomethyl ester **1c** and thionyl chloride [31].

Since two functionalities are present in these molecules, two different biocatalytic approaches were considered, the first involving hydrolysis of the ester group in the hydroxyesters and the second involving acylation of the hydroxyl group in the hydroxystearic acids, in organic solvent.

In particular, the resolutions of the hydroxyester **4d** and the hydroxystearic acids **5a–d** were first studied by computational analysis to verify the feasibility of their enantiodifferentiation by CALB and by lipase from *P. cepacia*.

2.1. Computational analysis: CALB enantiodiscrimination by exploiting the reactivity of the acyl group in 10-HSA methyl ester 4d

Trying to describe how the acylic pocket of CALB recognizes the enantiomers of the ester **4d**, a semi-quantitative approach was used to evaluate a possible energy difference in the tetrahedral reaction intermediates, by comparing, for each enantiomer, the distribution of the molecular dynamic (MD) poses stabilized by a certain number of H-bonds able to stabilize the oxy-anion hole and to allow the evolution to the subsequent reaction steps. In fact, it is known that the *R*- and *S*-enantiomers have different orientations to fulfil the necessary network of hydrogen bonds in transition state when reacting with CALB [32]. In the present study the computational analysis was performed in four steps (see also Section 4): (1) building up the tetrahedral intermediates inside the CALB active site; (2) conformational search to identify the lower energy conformation of substrate acyl chain; (3) equilibration by molecular dynamic simulation; (4) scoring of tetrahedral intermediates by analysing H-bond pattern. An analogous approach was then followed also for lipase from *P. cepacia* [33]. When one of the two enantiomers is stabilized at a higher extent, a difference in activation energy between the reactions of the two reactions is expected, which ultimately translates into enantiodiscrimination. As an example, Part (C) of Fig. 1 shows the H-bond profiles for the tetrahedral intermediate (i.e. transition state analog) of enantiomers of 1,2-dimethylpropyl octanoate, whose resolution with CALB leads to $E > 700$ [28]. It is evident that the (*R*)-enantiomer presents a higher number of "poses" stabilized by 3–5 H-bond, whereas the slow reacting (*S*)-enantiomer has a higher chance to be stabilized by only one or two H-bonds. Therefore, statistically speaking, there is a higher number of conformational poses of the tetrahedral intermediate of (*R*)-enantiomer having lower energy and being more reactive.

Data reported in Fig. 1A and B show that the poses of tetrahedral intermediates of both enantiomers of ester **4d** establish similar numbers of H-bonds inside the active sites of the two lipases here considered. Therefore, the tetrahedral intermediates of the enantiomers will be stabilized at a similar extent, leading to comparable reaction rates. As a conclusion, enantiodiscrimination seems unfeasible for substrate **4d** by using either CALB or lipase from *P. cepacia*. Therefore, this preliminary study clearly indicates that the "natural" reactivity of the carboxyl group cannot be exploited for the enantioresolution of the HSA ester **4d**.

2.2. Computational analysis: CALB substrate recognition and reactivity on the secondary OH group in 7-, 8-, 9-, and 10- HSA 5a–d

We recently constructed a 3D-QSAR model able to describe and predict the enantioselectivity of CALB [29]. The application of the 3D-QSAR model previously developed implies a number of computational steps: (a) calculation of the active conformers of the tetrahedral intermediates for all enantiomers of **5a–d** by molecular

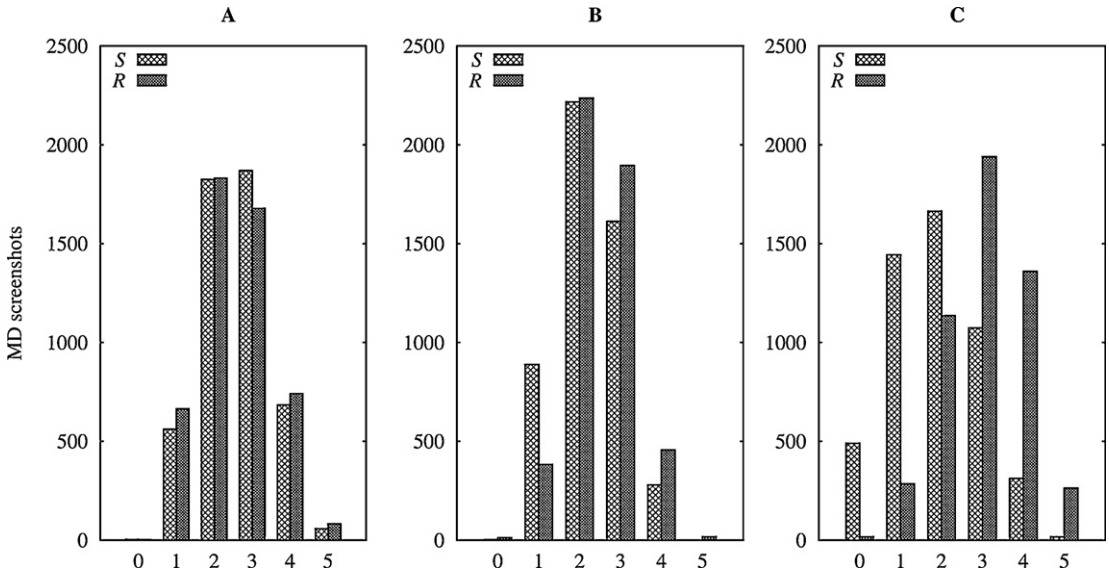

Fig. 1. Distribution of poses of the tetrahedral intermediates of enantiomers stabilized by a defined number of H-bonds. (A) Tetrahedral intermediate of **4d** in CALB; (B) tetrahedral intermediate of **4d** in lipase from *Pseudomonas cepacia*; (C) tetrahedral intermediate of 1,2-dimethylpropyl octanoate in CALB. X axis represents the number of H-bonds established by the substrate inside the acylic pocket. Y axis expresses the frequency of a specific molecular dynamic pose characterized by a certain number of stabilizing H-bonds.

dynamics simulations; (b) generation of the molecular descriptors for the pairs of enantiomers by means of GRID analysis and DMIF calculation; (c) calculation of the *E* value from the 3D-QSAR regression model (PLS partial least squares – projection to latent structures) [29].

Initially, it was necessary to model the tetrahedral intermediates for enantiomers of substrates **5a–d**. However, a preliminary study of docking of the substrate ground state into the alcohol pocket, by using the docking algorithm AlphaPMI, was unable to produce reliable poses consistent with catalysis. HSAs are characterized by a high number of rotatable bonds that result into an exceeding conformational freedom. Because of the various rotatable bonds, the substrates got coiled in the funnel shaped active site, thus producing no pose. Attempts to modify the placement algorithm failed basically because, in agreement with the CALB biological role, the carboxylic group of **5a–d** is better accommodated in the acylic pocket rather than in the alcohol pocket (see Fig. S1 in Supplementary Material).

To overcome these limitations and to model reliable tetrahedral intermediates, a pharmacophoral based approach (see Section 4) was applied by placing C1-decarboxylated derivatives of HSA acyl esters into the active site and by imposing a conformation compatible with catalysis (Fig. S2 in Supplementary Material). Afterwards the structure of the models was completed by reintroducing the carboxylic moiety on C1 and constructing the tetrahedral intermediates from the acetic ester moiety.

A molecular dynamic simulation was performed in order to relax the tetrahedral intermediates and evaluate the structures to be used in the 3D-QSAR model (300 ps, NVT, freezing atoms more than 10 Å far away from the TI).

It must be noted that both chains bounded to the alcohol moiety are too long and bulky to be accommodated freely inside the stereospecificity pocket. Interestingly, the MD relaxation showed some enlargement and conformational adaptations of the active site funnel for accommodating such bulky substrates. Although the short MD simulation did not allow any conclusive analysis of the conformational behaviour of CALB in the presence of HSA substrates, the observation suggests that a movement of α-10 helix [34], might enable a better substrate binding (upper simulation of Fig. 2). However, the consequent displacement of the loop corresponding to residues Glu188 and Ile189, on the contrary, would lead to a wrong displacement of Asp187 from the catalytically productive conformation (lower simulations of Fig. 2). Therefore, these discrepant observations cannot lead to any conclusive prevision of CALB reactivity to HSAs and indicate that Kazlauska's rule cannot be applied

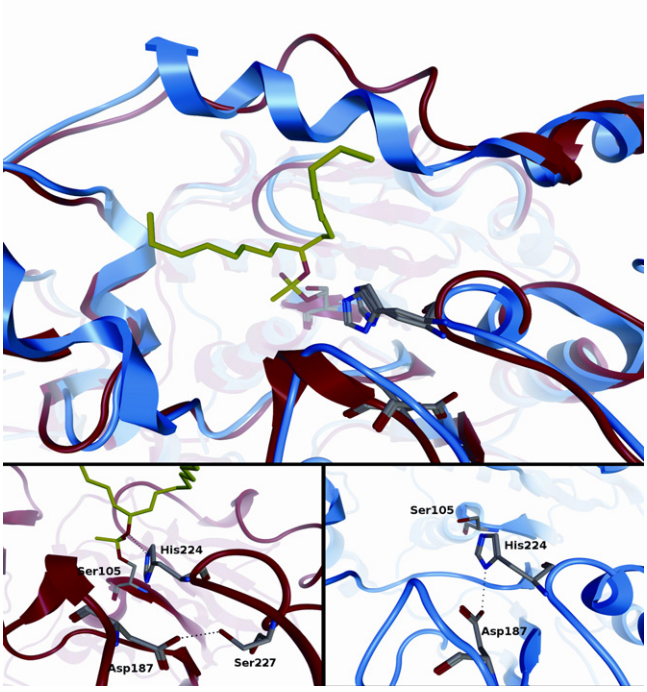

Fig. 2. Displacement of Asp187 and partial unfolding of α-10 helix enlarges the alcohol pocket of CALB active site. Crystallographic structure of CALB (1LBT) is in blue and final MD snapshot in red. The small frame on the right (blue) shows the productive position of the three aminoacids of the catalytic triad, with Asp187 forming a H-bond with His224. The frame on the left (red) illustrates the displacement of Asp187 as a result of the fitting of the bulky hydroxyacyl moiety inside the stereospecificity pocket. Conversely, Asp187 cannot interact with His224 in a productive way. (For interpretation of the references to color in this figure legend, the reader is referred to the web version of the article.)

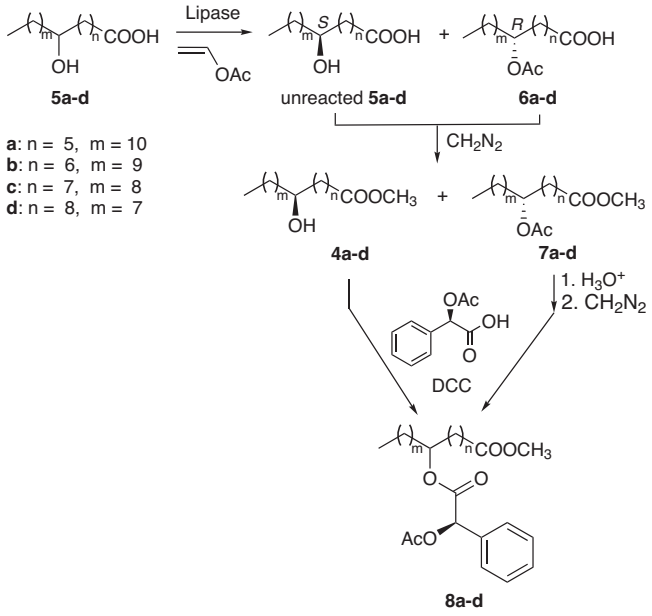

Scheme 2. Lipase catalysed acylation of hydroxystearic acids **5a**–**d**.

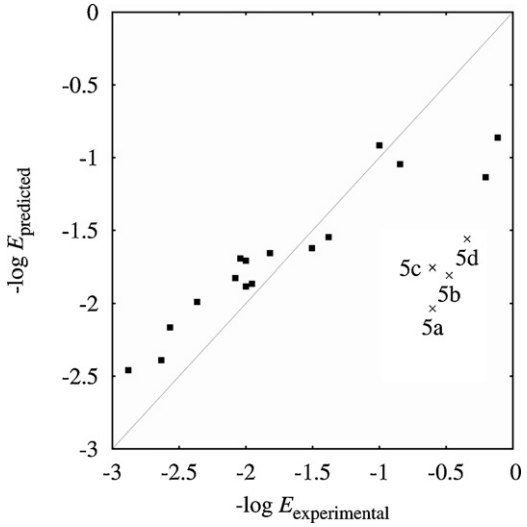

Fig. 3. Predictivity of the model in terms of experimental versus predicted *E* values. Objects taken from the training set of the PLS model are represented by squares. The performance of the model towards four HSAs, **5a**–**b**, is highlighted by crosses.

to HSA acyl esters. By applying the cited 3D-QSAR approach to **5a**–**d**, the model predicted an enantiopreference towards the (*R*) enantiomer. However, the indications obtained from the 3D-QSAR model induced to test this type of reactivity looking for, at least, some enantiomeric enrichment.

2.3. Experimental results

Lipase catalysed hydrolysis of methyl 10-hydroxystearate **4d**.

As a confirmation of the theoretical evaluations, both lipases are able to catalyse the hydrolysis of methyl 10-hydroxystearate **4d** (Table 1) with acceptable reaction rate but with low enantioselectivity, as shown by their very low *E* values.

2.4. Lipase catalysed acylation of hydroxystearic acids *5a–d* with CALB and PS

The experimental results of lipase catalysed acylations carried out on the HSAs **5a**–**d** using lipase B from *C. antarctica* (CALB) and lipase from *P. cepacia* "Lipo P. Cepacia" (PS) with vinyl acetate as the acylating agent are reported in Scheme 2 and Table 2.

Reactions were monitored by ^{1}H NMR, following the appearance of a quintet at about 4.8 ppm relative to the CHOAc protons of the acetoxy acids **6a**–**d**. The e.e.'s of both **5a**–**d** and **6a**–**d** were determined following a complex procedure shown in Scheme 2. The reaction mixtures containing the unreacted hydroxyacids **5a**–**d** and the reaction products **6a**–**d** were treated with diazomethane to esterify both carboxylic groups. The resulting derivatives **4a**–**d** and **7a**–**d**, respectively were separated by preparative TLC and separately derivatized with (*R*)-(−)-*O*-acetylmandelic acid, the latter compound after hydrolysis and esterification (Scheme 2). The resulting diastereomeric acetylmandelate derivatives **8a**–**d** were then analysed by 600 MHz ^{1}H NMR to determine the enantiomeric excesses of the parent compounds **5a**–**d** and **6a**–**d**. The absolute configurations of **8a** and **8d**, derived from the unreacted hydroxyacids **5c** and **5d**, were (9S,2′R) and (10S,2′R), respectively [16a,36]. In fact, these latter compounds were the major components in their respective diastereomeric mixtures. As a consequence, the parent hydroxyacids **5c** and **5d** are (*S*)-9-HSA and (*S*)-10-HSA and the acetoxyacids **6c** and **6d** must be (*R*). An analogous determination could not be made for **5a** and **5b** and their absolute configurations were tentatively assigned as (*S*) for analogy.

Experimental data clearly show that CALB is able to acylate the —OH group of HSAs despite a very low catalytic efficiency, as predicted by docking studies. Since the substrates are too bulky for being accommodated in the stereospecific alcohol pocket, some induced fit of CALB might be involved in the enzyme-substrate recognition, although extensive MD simulation would be necessary to explore this hypothesis in further detail.

As for enantioselectivity, modest enantiodiscrimination was observed. The indications gained from the 3D-QSAR model were correct in term of prediction of the fast reacting enantiomer but a clear overestimation of enantioselectivity was done by the model (Fig. 3) due to the diversity between acetoxystearic acids and the data set used to train the 3D-QSAR model.

As it can be seen in Table 2, calculated and measured conversion values were similar with the exception of those reported for **5d** in its reaction with CALB. As expected on the basis of the substrate structures, *E* values were low for all reactions and consequently the optical purity of the products were not high, ranging from 16 to 56%.

Acylation reactions carried out with lipase PS were less satisfactory and only two results are reported in Table 2, namely those relative to compounds **5c** and **5d**.

Interestingly, the acylation reaction carried out on the esters **4a**–**d** did not proceed, most probably because the enzyme recognizes the fatty ester leading to an acyl enzyme that, however, has no nucleophile available for being transformed at a reasonable rate. Indeed, the water activity is too low. As a matter of fact, the ester is a more active acylating agent as compared to the carboxylic acid. When the HSA enters the acylic pocket it hardly react with the catalytic Ser105, so that it has a chance to leave the acylic pocket unreacted and then to interact with the enzyme according different modalities.

It is likely that also the ester fits preferentially inside the acylic pocket (as the acid does). In that case the catalytic Ser105 gets acylated and ethanol is released but no further nucleophile is available in the reaction environment to attack the acyl-enzyme. In fact, the HAS is too bulky to be accommodated inside the active site next the acyl-enzyme. Therefore the acyl-enzyme is not transformed. As a consequence, the HSA ester is not available for being acylated on the —OH group.

Table 1
Lipase catalysed hydrolyses of methyl 10-hydroxystearate **4d**.

Enzyme	Time (d)	Conv. (%)[a]	Unreacted substrate **4d** e.e.$_s$ (%)[b]	E[c]
CALB[d]	2.5	58	12	1.3
PS	2.5	50	7	1.2

[a] Determined by ^{1}H NMR analysis.
[b] Determined by integration of the methoxy signal in the 600 MHz ^{1}H NMR spectrum of diastereomeric (*R*)-(−)-*O*-acetylmandelate esters (see infra).
[c] $E = \frac{\ln[(1-c)(1-\text{e.e.}_s)]}{\ln[(1-c)(1+\text{e.e.}_s)]}$; Ref. [35].
[d] Novozym 435 and LipoCALB gave the same results.

3. Conclusions

The structural anomaly of hydroxystearic acids is the presence of a chiral carbon on the acyl moiety, which make difficult the application of general rules in the prediction of CALB enantiopreference. As a matter of fact, the acyl moiety is accommodated into the acyl pocket of CALB which is not responsible for enantiodiscrimination. Indeed, the Kazlauskas's rule as well as the 3D-QSAR model previously developed for predicting CALB enantiodiscrimination are strictly connected to the structural features of the alcohol pocket of CALB. Hydroxy fatty acids are acylated very slowly by lipase from *C. antarctica* due to the preferred fitting of the carboxyl group into the acyl pocket of the enzyme. Because of the bulky alcohol moiety, the stereospecific pocket cannot host the substrates and thus these secondary alcohols do not follow either Kazlauskas' rule or 3D-QSAR models predicting enzyme enantioselectivity. Modelling study illustrated clearly how enantiodiscrimination is not feasible by exploiting the reactivity of the acylic group, although reactions are faster through this route. The accommodation of the acyl chain causes conformational distortion of the alcohol pocket (Fig. 2). Therefore the substrate recognition occurs according different criteria as compared "normal" alcohols because in the case of HAS the —OH group is hardly positioned in the right pocket.

However, this is the first attempt to get to enantioenriched hydroxystearic acids by the use of enzymatic resolution. Although we are conscious of the challenge, these first results seem promising: two hydroxyacids, namely (*R*)-7-HSA and (*S*)-9-HSA were obtained with about 55% e.e., the former after hydrolysis of its acetylated derivative. In spite of the poor enantiomeric excesses, it is our opinion that biological tests would still be worth performing, in order to have an indication of the influence of the absolute configuration on the biological activity of the molecules.

4. Experimental

4.1. General

Lipase from *C. antarctica* "Novozym 435", ≥10,000 U/g (Novo Nordisk A/S, Bagsvaerd, Denmark), lipase from *C. antarctica* (Lipo CALB), ≥2000 U/g (Sprin Technologies S.p.A., Trieste, Italy) and lipase from *P. cepacia* "Lipo P. Cepacia" (PS), ≥100 U/g (Sprin Technologies S.p.A., Trieste, Italy) were used.

Nonanedioic acid, 1-methyl ester (**1c**), methyl 8-chloro-8-oxooctanoate (**2b**), methyl 7-oxooctadecanoate (**3a**), methyl 10-oxooctadecanoate (**3d**) and *n*-decyl magnesium bromide (1.0 M in diethyl ether) were purchased from Sigma–Aldrich (Milan, Italy). Methyl 9-oxooctadecanoate (**3c**) was prepared according to the literature [12c]. Anhydrous THF was prepared by distillation over sodium benzophenone ketyl. Thin-layer chromatography (TLC) was carried out using silica gel precoated on TLC Alu foils from Fluka and spots were revealed using an aqueous solution of $(NH_4)_6MoO_{24}$ (25%), $(NH_4)_4Ce(SO_4)_4$ (1%) in 10% H_2SO_4 as staining reagent. For preparative TLC, 20 × 20 silica gel plates (Merck Kieselgel 60F_{254}) were used. Flash chromatography was run on silica gel 230–400 mesh ASTM (Kieselgel 60, Merck). Light petroleum refers to the fraction with b.p. 40–70 °C. ^{1}H and ^{13}C NMR spectra were recorded on a Varian Mercury 400 or an Inova 300 or 600 spectrometer (Varian, Palo Alto, CA). Frequencies are reported in Hz and chemical shifts in ppm are referred, if not otherwise specified, to the solvent: $CDCl_3$ (δ = 7.27 ppm for ^{1}H NMR and δ = 77.0 ppm for ^{13}C NMR). Signal multiplicities were assigned by DEPT experiments. EI and HRMS mass spectra were recorded using a VG-7070E spectrometer at an ionization voltage of 70 eV. ESI-MS spectra were recorded on a WATERS 2Q 4000 instrument. IR spectra were recorded using a Perkin-Elmer FT-IR MOD.1600 spectrophotometer. Melting points were measured by a Büchi apparatus and were not corrected.

4.2. Synthesis of substrates

4.2.1. Methyl 8-oxooctadecanoate (*3b*)

A solution of *n*-decyl magnesium bromide (1 M in diethyl ether, 15.05 mL) was added, under nitrogen atmosphere, to a solution of methyl 8-chloro-8-oxooctanoate (**2b**, 3.11 g, 15.05 mmol) cooled at −78 °C. After 5 min the reaction mixture was treated with water (20 mL) and the organic layer was separated. The aqueous layer was extracted with diethyl ether (3× 20 mL). The organic layers were washed with 'brine' then dried over anhydrous $MgSO_4$. After filtration and removal of the solvent under reduced pressure, the residue

Table 2
Acetylation of hydroxystearic acids **5a**–**d** mediated by CALB and PS.

Enzyme	Substrate	Time (d)	Conv. (%), calc.[a]	Conv. (%), by ^{1}H NMR	Unreacted substrates **5a**–**d** e.e.$_s$ (%)[b]	Acetylated acids **6a**–**d** e.e.$_p$ (%)[b]	E[c]
Novozym 435	**5a**	14	15	13	10[d]	56[d]	4
Novozym 435	**5b**	7	39	32	24[d]	38[d]	3
Novozym 435	**5c**	5	56	53	54[d]	42[d]	4
Novozym 435	**5d**	7	46	37	24[e]	28[e]	2.2
PS	**5c**	7	–	37	30[e]	–	4[f]
PS	**5d**	7	50	34	16[e]	16[d]	1.6

[a] $c = \frac{\text{e.e.}_s}{\text{e.e.}_s+\text{e.e.}_p}$
[b] Determined by 600 MHz ^{1}H NMR analysis of diastereomeric (*R*)-(−)-*O*-acetylmandelate esters of the methyl ester derivatives **8a**–**d**.
[c] $E = \frac{\ln[\text{e.e.}_p(1-\text{e.e.}_s)]/(\text{e.e.}_p+\text{e.e.}_s)}{\ln[\text{e.e.}_p(1+\text{e.e.}_s)]/(\text{e.e.}_p+\text{e.e.}_s)}$; Ref. [35].
[d] Determined by integration of H-2′ signals of (*R*)-(−)-*O*-acetylmandelate derivatives.
[e] Determined by integration of the methoxy group signals of (*R*)-(−)-*O*-acetylmandelate derivatives.
[f] $E = \frac{\ln[(1-c)(1-\text{e.e.}_s)]}{\ln[(1-c)(1+\text{e.e.}_s)]}$; Ref. [35].

was purified by flash-chromatography (light petroleum/diethyl ether 4/1); 1.0 g, (21%) of **3b** was obtained. m.p.: 45–46 °C (lit.: [37] 46.4–46.9 °C). ^{1}H NMR (400 MHz, $CDCl_3$) δ (ppm): 3.46 (s, 3H, OCH_3), 2.20 (t, J = 7.5 Hz, 2H, CH_2CO), 2.19 (t, J = 7.5 Hz, 2H, CH_2CO), 2.10 (t, J = 7.5 Hz, 2H, CH_2CO), 1.55–1.25 (m, 6 H), 1.25–0.99 (m, 18 H), 0.69 (t, J = 6.8 Hz, 3H, CH_3); ^{13}C NMR (100.56 MHz, $CDCl_3$) δ (ppm): 210.2, 173.4, 50.8, 42.3, 42.1, 33.4, 31.5, 29.2, 29.1, 29.0, 28.90, 28.85, 28.5, 28.4, 24.3, 23.4, 23.1, 22.2, 13.6; MS (m/z), (%): 312 (M^+, 2), 281 (15), 239 (9), 199 (8), 184 (56), 171 (76). 154 (61), 144 (70), 129 (100), 111 (67), 97 (56), 83 (70), 69 (61), 55 (78).

4.2.2. Methyl hydroxyoctadecanoates **4a–d**

Compounds **4a–d** were prepared from the corresponding ketone precursor following the procedure reported for the preparation of **4c** and **4d** [12c]. Characterization data of compounds **4a–d** agree with those reported in the literature [12c,37–39]. The new spectral data are reported below.

4.2.3. Methyl 7-hydroxyoctadecanoate (**4a**) [37,38]

^{1}H NMR (600 MHz, $CDCl_3$) δ (ppm): 3.67 (s, 3H, OCH_3), 3.62–3.56 (m, 1H, C*H*OH), 2.32 (t, J = 7.5 Hz, 2H, CH_2CO), 1.68–1.60 (m, 2H), 1.51–1.22 (m, 27H), 0.89 (t, J = 7.0 Hz, 3H, CH_3); MS (m/z), (%): 296 (0.4), 264 (7), 159 (35), 127 (100), 87 (76).

4.2.4. Methyl 8-hydroxyoctadecanoate (**4b**) [37–39]

M.p.: 54–55 °C (lit.: [39a] 54.5–55.5 °C). ^{1}H NMR (400 MHz, $CDCl_3$) δ (ppm): 3.65 (s, 3H, OCH_3), 3.60–3.51 (m, 1H, C*H*OH), 2.29 (t, J = 7.6 Hz, 2H, CH_2CO), 1.68–1.16 (m, 29H), 0.87 (t, J = 6.7 Hz, 3H, CH_3); MS (m/z), (%): 296 (0.4), 264 (3), 173 (35), 141 (100).

4.2.5. Hydroxyoctadecanoic acids **5a–d**

Compounds **5a–d** were prepared from the corresponding methyl ester following the procedure reported [14] for the preparation of 9-hydroxylstearic acid **5c**. Characterization data of compounds **5a–d** agree with those reported in the literature [12c,37]. The new spectral data are reported below.

4.2.6. 7-Hydroxyoctadecanoic acid (**5a**) [40]

^{1}H NMR (400 MHz, $CDCl_3$) δ (ppm): 3.70–3.52 (m, 1H, C*H*OH), 2.37 (t, J = 7.6 Hz, 2H, CH_2CO), 1.74–1.59 (m, 2H), 1.53–1.21 (m, 27H), 0.89 (t, J = 6.7 Hz, 3H, CH_3); ^{13}C NMR (100.56 MHz, $CDCl_3$) δ (ppm): 177.4, 71.9, 37.5, 37.2, 33.5, 31.9, 29.69, 29.66, 29.63 (two overlapping signals), 29.61, 29.3, 29.1, 25.6, 25.3, 24.6, 22.7, 14.1.

4.2.7. 8-Hydroxyoctadecanoic acid (**5b**) [37,41]

^{1}H NMR (400 MHz, $CDCl_3$) δ (ppm): 3.63–3.55 (m, 1H, C*H*OH), 2.35 (t, J = 7.4 Hz, 2H, CH_2CO), 1.69–1.59 (m, 2H), 1.51–1.22 (m, 27H), 0.89 (t, J = 6.7 Hz, 3H, CH_3); ^{13}C NMR (100.56 MHz, $CDCl_3$) δ (ppm): 179.3, 72.0, 37.5, 37.3, 33.9, 31.9, 29.7, 29.6 (three overlapping signals), 29.3, 29.25, 29.0, 25.6, 25.4, 24.6, 22.7, 14.1.

4.2.8. 9-Hydroxyoctadecanoic acid (**5c**) [37]

^{1}H NMR (400 MHz, $CDCl_3$) δ (ppm): 3.66–3.54 (m, 1H, C*H*OH), 2.37 (t, J = 7.8 Hz, 2H, CH_2CO), 1.69–1.60 (m, 2H), 1.60–1.23 (m, 27H), 0.89 (t, J = 7.0 Hz, 3H, CH_3); ^{13}C NMR (100.56 MHz, $CDCl_3$) δ (ppm): 178.7, 72.0, 37.5, 37.4, 33.5, 31.9, 29.7, 29.65, 29.58, 29.5, 29.3, 29.2, 29.0, 25.7, 25.5, 24.7, 22.7, 14.1.

4.2.9. 10-Hydroxyoctadecanoic acid (**5d**) [37,41]

^{1}H NMR (300 MHz, $CDCl_3$) δ (ppm): 3.67–3.50 (m, 1H, C*H*OH), 2.34 (t, J = 7.5 Hz, 2H, CH_2CO), 1.69–1.23 (m, 29H), 0.88 (t, J = 7.2 Hz, 3H, CH_3); ^{13}C NMR (100.56 MHz, $CDCl_3$) δ (ppm): 178.8, 72.1, 37.4 (two overlapping signals), 33.9, 31.9, 29.8 (2), 29.6 (2), 29.3, 29.1, 29.0, 25.6, 25.5, 24.6, 22.7, 14.1.

4.3. Enzymatic hydrolysis of methyl 10-hydroxystearate **4d**

To 0.060 g (0.2 mmol) of **4d**, 1 mL of acetone, 9 mL of 0.1 M phosphate buffer ($NaHPO_4/KH_2PO_4$) at pH 7.4 and 0.060 g of the lipase Novozym 435 or Lipo CALB or PS was added. After 2.5 days the aqueous suspension was filtered off through a Gooch funnel to recover the enzyme and the mother liquors were extracted four times with diethyl ether and dried over anhydrous Na_2SO_4. Both the hydroxyacid **5d** and its methyl ester **4d** were extracted at pH 7.4 and the mixture was analysed by ^{1}H NMR. Conversions were determined by integration of the signals at 3.59 ppm (bs, H-10 of **4d** and **5d**) and at 3.68 ppm (s, CH_3O of **4d**). The ester **4d** was separated from the acid **5d** by flash chromatography (petroleum ether/ethyl acetate: 9/1, 25% yield) and the hydroxyl group was esterified with (*R*)-(−)-*O*-acetylmandelic acid [16b]. The enantiomeric excess of the unreacted substrate was calculated from the ^{1}H NMR (600 MHz) spectrum of the mixture of the two diastereomers **8d** obtained which agreed with previously reported data [16b,36].

4.4. Lipase catalysed acylations of hydroxystearic acids **5a–d**

To 0.070 g (0.23 mmol) of hydroxystearic acid, 3 mL of vinyl acetate, 4 mL of diethyl ether and 0.070 g of Novozym 435 or Lipo P. Cepacia (PS) were added. The mixture was stirred at room temperature for 5–14 days. The suspension was filtered through a Gooch funnel, the enzyme was washed with diethyl ether and the solvent was evaporated. Conversions were determined by integration of the signals at about 3.6 ppm (bs, C*H*OH of **5a–e**) and at about 4.8 ppm (quintet, C*H*OAc of **6a–d**) of the ^{1}H NMR spectrum (in $CDCl_3$) of the crude reaction mixture. This latter was dissolved in the minimum amount of methanol and esterified 'in situ' with diazomethane in diethyl ether using Aldrich® diazomethane-generator apparatus. After removal of the solvent, preparative TLC (light petroleum/diethyl ether: 7/3) of the residue allowed to separate compounds **4** ($R_F \sim 0.25$) and **7** ($R_F \sim 0.7$). The related scraped silica gel bands were suspended and stirred in methanol, giving, after filtration and removal of the solvent, compounds **4** and **7**. The hydroxy group of the methyl hydroxyester (**4a–d**) thus obtained was esterified with (*R*)-(−)-*O*-acetylmandelic acid [16b] to determine the enantiomeric excess of the unreacted substrate by ^{1}H NMR. The methyl acetoxyoctadecanoates (**7a–d**) were dissolved in methanol (1–2 mL) and treated with an excess (1.0–2.0 mL) of 10% KOH/CH_3OH. The solution was magnetically stirred at room temperature and monitored by TLC (light petroleum/diethyl ether: 7/3) until complete disappearance of the starting material. The flask was immersed in an ice-bath and the solution was acidified by adding dropwise 37% aq. HCl solution. After filtration, the methanol was partially removed and the residue containing the hydroxyacid was treated with diazomethane in diethyl ether. The solvent was removed and the residue was treated with (*R*)-(−)-*O*-acetylmandelic acid following the reported procedure [16b] to determine the enantiomeric excess of **6a–d** by ^{1}H NMR. The new spectral data for compounds **7a–d** and **8a**,**b** are reported below, while spectral data for **8c** and **8d** are consistent with those reported in the literature [16b,36].

4.4.1. Methyl 7-acetoxyoctadecanoate (**7a**) [38a,38d,42]

^{1}H NMR (400 MHz, $CDCl_3$) δ (ppm): 4.85 (quintet, 6.7 Hz, 1H), 3.67 (s, 3H, OCH_3), 2.30 (t, J = 7.7 Hz, 2H), 2.04 (s, 3H, CH_3CO), 1.67–1.58 (m, 2H), 1.56–1.46 (m, 4H), 1.38–1.20 (m, 22H), 0.89 (t, J = 7.0 Hz, 3H, CH_3).

4.4.2. Methyl 8-acetoxyoctadecanoate (**7b**) [38a,38d]

^{1}H NMR (400 MHz, $CDCl_3$) δ (ppm): 4.86 (quintet, 6.5 Hz, 1H), 3.68 (s, 3H, OCH_3), 2.31 (t, J = 7.5 Hz, 2H), 2.04 (s, 3H, CH_3CO),

1.66–1.59 (m, 2H), 1.54–1.48 (m, 4H), 1.35–1.22 (m, 22H), 0.89 (t, J = 7.2 Hz, 3H, CH_3).

*4.4.3. Methyl 9-acetoxyoctadecanoate (**7c**) [38a,38d,43]*

^{1}H NMR (400 MHz, $CDCl_3$) δ (ppm): 4.86 (quintet, 6.5 Hz, 1H), 3.67 (s, 3H, OCH_3), 2.30 (t, J = 7.7 Hz, 2H), 2.04 (s, 3H, CH_3CO), 1.66–1.56 (m, 4H), 1.55–1.46 (m, 4H), 1.35–1.22 (m, 20H), 0.89 (t, J = 6.7 Hz, 3H, CH_3).

*4.4.4. Methyl 10-acetoxyoctadecanoate (**7d**) [38a,38d]*

^{1}H NMR (400 MHz, $CDCl_3$) δ (ppm): 4.84 (quintet, 6.6 Hz, 1H), 3.66 (s, 3H, OCH_3), 2.29 (t, J = 7.5 Hz, 2H), 2.03 (s, 3H, CH_3CO), 1.65–1.57 (m, 2H), 1.53–1.46 (m, 4H), 1.32–1.20 (m, 22H), 0.87 (t, J = 7.2 Hz, 3H, CH_3).

*4.4.5. Methyl (7R)-7-{[(2R)-2-(acetyloxy)-2-phenylacetyl]oxy}octadecanoate and methyl (7S)-7-{[(2R)-2-(acetyloxy)-2-phenylacetyl]oxy}octadecanoate (**8a**)*

Within the mixture containing different relative amounts of two diastereomers, indicated as **diast1-8a** and **diast2-8a**, it was possible to distinguish some signals of each and consequently to describe the related spectrum. **diast1-8a**: ^{1}H NMR (600 Mz, $CDCl_3$, TMS) δ (ppm): 7.47 (dd, J = 7.8 Hz, J = 2.2 Hz, 2H), 7.41–7.31 (m, 3H), 5.869 (s, 1H, CHPh), 4.91–4.84 (m 1H), 3.657 (s, 3H, OCH_3), 2.158 (t, J = 7.6 Hz, 2H, H-2), 2.20 (s, 3H, CH_3CO), 1.70–0.99 (m, 28H), 0.883 (t, J = 7.2 Hz, 3H, CH_3); **diast2-8a**: ^{1}H NMR (600 Mz, $CDCl_3$, TMS) δ (ppm): 7.47 (dd, J = 7.8 Hz, J = 2.2 Hz, 2H), 7.41–7.31 (m, 3H), 5.861 (s, 1H, CHPh), 4.91–4.84 (m 1H), 3.662 (s, 3H, OCH_3), 2.289 (t, J = 7.6 Hz, 2H, H-2), 2.20 (s, 3H, CH_3CO), 1.70–0.99 (m, 28H), 0.888 (t, J = 7.2 Hz, 3H, CH_3).

*4.4.6. Methyl (8R)-8-{[(2R)-2-(acetyloxy)-2-phenylacetyl]oxy}octadecanoate and methyl (8S)-8-{[(2R)-2-(acetyloxy)-2-phenylacetyl]oxy}octadecanoate (**8b**)*

From the mixture containing different relative amount of the two diastereomers, indicated as **diast1-8b** and **diast2-8b**, it was possible to distinguish some signals of each and consequently to describe the related spectrum. **diast1-8b**: ^{1}H NMR (600 Mz, $CDCl_3$, TMS) δ (ppm): 7.51–7.45 (m, 2H), 7.43–7.33 (m, 3H), 5.872 (s, 1H, CHPh), 4.91–4.84 (m 1H), 3.666 (s, 3H, OCH_3), 2.239 (t, J = 7.6 Hz, 2H, H-2), 2.20 (s, 3H, CH_3CO), 1.70–0.99 (m, 28H), 0.885 (t, J = 7.2 Hz, 3H, CH_3); **diast2-8b**: ^{1}H NMR (600 Mz, $CDCl_3$, TMS) δ (ppm): 7.51–7.45 (m, 2H), 7.43–7.33 (m, 3H), 5.867 (s, 1H, CHPh), 4.91–4.84 (m 1H), 3.665 (s, 3H, OCH_3), 2.295 (t, J = 7.6 Hz, 2H, H-2), 2.20 (s, 3H, CH_3CO), 1.70–0.99 (m, 28H), 0.890 (t, J = 7.2 Hz, 3H, CH_3).

4.5. Modelling H-bonding stabilization of tetrahedral intermediates

The computational analysis was performed starting from the crystal structures of CALB (PDB code: 1TCA) and PS (PDB code: 4LIP) properly pretreated removing glycans and solvents. Both protein structures were protonated (pH 7) and then relaxed by a molecular dynamic simulation (300 K, 1000 ps, implicit solvent, NVT ensemble). All the computation was performed with Molecular Operating Environment suit (MOE2009.10 – Chemical Computing Group - Montreal, Canada) using the Amber99 force field.

The tetrahedral intermediates for the reactions involving the terminal carboxylic moiety, were constructed by creating the covalent bond between the catalytic serine side chain and the substrate best productive poses of docking simulations (AlphaPMI placement, London dG re-scoring). The new bond was placed and the atom partial charges corrected and afterwards, the whole system was submitted to a local energy minimization (including atoms in 6 Å radius from the tetrahedral carbon) and finally to a global energy minimization (until gradient less than 0.01 kcal/mol). Since the fatty acid chain consists of several rotatable bonds, a conformational search was performed with the low mode MD conformational search tool of MOE. The lowest potential energy conformation was chosen and then energy minimized producing the final tetrahedral intermediate.

The analysis of the H-bond pattern was performed by means of the in-house developed SVL tool (Scientific Vector Language in MOE2009.10) based in molecular dynamic simulations by using an adequate time of equilibration (energy gradient less than 0.05 kcal/mol in the last 100 ps) and productive time of 1000 ps (time step 0.2 ps, 300 K, implicit solvent, NVT ensemble). For each of the 5000 sampled conformations, the tool calculated the number of H-bonds involving one of the three oxygen atoms directly connected with the tetrahedral carbon of the intermediate. Only those H-bonds that can contribute to the stabilization of intermediates were taken into account (oxyanion–oxyanion hole, alcohol moiety deriving oxygen–nitrogen of His side chain, Ser side chain oxygen–nitrogen of His side chain). The resulting profile shows the occurrence of poses stabilized by a defined number of H-bonds which were observed during the production MD step.

4.6. Modelling of tetrahedral intermediates of HSAs in the alcohol pocket of CALB

The docking of HSA substrates was not able to generate any reliable pose of the alcohol moiety of HSA in the active sites of both enzymes. Basically, all the placements algorithms implemented in MOE gave poses with the carboxyl functionality close to the catalytic machinery and, conversely, the hydroxy group out of the deeper active site region. To obtain a structural model of the tetrahedral intermediates having HSA as acyl acceptor, a decarboxylated acetyl ester derivative was docked using a pharmacophoral based placement. The pharmacophore was designed introducing two requirements for the docking poses: the location of the carbonyl oxygen toward the oxyanion hole and a small hydrophobic moiety in the acyl pocket. Using this restrains the acetylated decarboxylated substrate was docked by imposing the ester group upon the catalytic machinery (Ser-His and oxyanion hole). After the placement of such decarboxylated substrates, the carboxyl group was added to the system in order to recover the wanted functionality of substrates. Afterwards, tetrahedral intermediates were built making the covalent bond with the enzyme, changing the atom charges and finally minimizing the energy until energy gradient less than 0.01 kcal/mol.

Since tetrahedral intermediates were built by forcing the substrate poses with the pharmacophoral placement, a relaxation of the system was required. Thus a molecular dynamic simulation was performed in order to relax the tetrahedral intermediates and evaluate the poses (300 ps, 300 K, implicit solvent, NVT, freezing atoms more than 10 Å far away from the tetrahedral intermediate).

4.7. 3D-QSAR

Differential Molecular Interaction Field (DMIF) has been used as descriptors for PLS model as already published [29]. The reliable structure of a couple of tetrahedral intermediates, the *R* and *S* enantiomers of the substrate under investigation, has been analysed calculating the molecular interaction field (MIF) with the software GRID (Molecular Discovery Ltd., United Kingdom) using 4 probes and taking into account a box surrounding the substrate as defined in the cited work. The resulting pair of MIF has been used to calculate differential molecular interaction field (DMIF) making the

difference between the MIF deriving from *R* enantiomer and the one from the *S* enantiomer. Finally the DMIF was used to make the enantioselectivity prediction performing an external PLS prediction with the software GOLPE (MIA s.r.l., Perugia, Italy)

Acknowledgements

This work has received funding from the European Community Seventh Framework Programme under the FP7-KBBE-2008-2B grant agreement no. 227279(IRENE project), from Alma Mater Studiorum – Università di Bologna (Fundamental Oriented Research (RFO) funds) and from Ministero dell'Istruzione, dell'Università e della Ricerca (MIUR) (Project PRIN 20078J9L2A_005: "New frontiers in the synthesis, reactions and applications of compounds containing heteroatoms").

Appendix A. Supplementary data

Supplementary data associated with this article can be found, in the online version, at http://dx.doi.org/10.1016/j.molcatb.2012.06.017.

References

[1] (a) F.D. Gunstone, Fatty Acid and Lipid Chemistry, Springer Verlag, Berlin, 1996; (b) A.J. Fulco, Prog. Lipid Res. 22 (1983) 133–160; (c) J.L. Harwood, N.J. Russell, Lipids in Plants and Microbes, Allen and Unwin, London, 1984.
[2] A. Sevanian (Ed.), Lipid Peroxidation in Biological Systems, The American Oil Chemists Society, 1988.
[3] (a) G.N. McDermott, in: D. Swern (Ed.), Miscellaneous Oil and Fat Products in Bailey's Industrial Oil and Fat Products, John Wiley &Sons, New York, 1982; (b) H.M. Teeter, L.E. Gast, E.W. Bell, J.C. Cowan, Ind. Eng. Chem. 45 (1953) 1777–1779; (c) M. Farroq, A. Ramli, S. Gul, N. Muhammad, J. Appl. Chem. 11 (2011) 1381–1385.
[4] (a) E.H. Pryde, L.H.K.D. Princen, Mukherjiee New Sources of Fats and Oils, American oil Chemists Society, Champaign, 1981; (b) M. Svensson, in: M. Kjellin, I. Johansson (Eds.), Surfactants from Renewable Resources, vol. 1, John Wiley & Sons, Chichester, UK, 2010; (c) U. Biermann, U. Bornscheuer, M.A.R. Meier, J.O. Metzger, H.J. Schäfer, Angew. Chem. Int. Ed. 50 (2011) 3854–3871.
[5] (a) Z.S. Petrović, I. Ivetković, D. Hong, X. Wan, W. Zhang, T. Abraham, J. Malsam, J. Appl. Polym. Sci. 108 (2008) 1184–1190; (b) T. Hamaguchi, M. Atsuhito, Plasticizer for biodegradable resin, US Patent US20060276575 (2006).
[6] (a) F.C. Naughton, J. Am. Oil Chem. Soc. 51 (1974) 65–71; (b) D. Thetford, Paint compositions, EP Patent 1,383,840 (2008); (c) A. Marrion, A.R. Marrion, in: R. Alistair, Marrion (Eds.), Binders for Conventional Coatings in the Chemistry and Physics of Coatings, vol. 1, RCS Publ., 2004, pp. 96–150.
[7] T.F. Tadros, C. Dederen, M.C. Taelman, Parfuemerie Kosmetik 78 (1997) 30–34.
[8] (a) T.V. Drovetskaya, W.H. Yu, E.F. Diantonio, S.L. Jordan, Hair styling and conditioning personal care films, US Patent US 2010/0247459 A1 (2010).; (b) G.A. Grissett, D.M. Keenan, F.A. Macedo, D.R. Williams, Fibrous toilette article, US Patent US 10/938,384 (2008).
[9] W. Schwab, R. Davidovich-Rikanati, E. Lewinsohn, Plant J. 54 (2008) 712–732.
[10] (a) F. Shahidi (Ed.), Nutraceutical and Specialty Lipids and Their Co-products, CRC Press, 2006; (b) N.E. Hughes, A.G. Marangoni, A.J. Wright, M.A. Rogers, J.W.E. Rush, Trends Food Sci. Technol. 20 (2009) 470–480; (c) J.F. Toro-Vazquez, J. Morales-Rueda, Food Biophys. 5 (2010) 193–202.
[11] (a) M.A. Rogers, A.J. Wright, A.G. Marangoni, Soft Matter 4 (2008) 1483–1490; (b) M.A. Rogers, A.J. Wright, A.G. Marangoni, Curr. Opin. Colloid Interface Sci. 14 (2009) 33–42; (c) M.A. Rogers, J.H.J. Kim, Food Res. Int. 44 (2011) 1447–1451; (d) L. Cristofolini, M.P. Fontana, C. Boga, O. Konovalov, Langmuir 21 (2005) 11213–11219.
[12] (a) L. Masotti, E. Casali, N. Gesmundo, G. Sartor, T. Galeotti, S. Borrello, M.V. Piretti, G. Pagliuca, Ann. N. Y. Acad. Sci. 51 (1989) 47–58; (b) L. Masotti, E. Casali, N. Gesmundo, Mol. Aspects Med. 14 (1993) 209–215; (c) C. Bertucci, M. Hudaib, C. Boga, N. Calonghi, C. Cappadone, L. Masotti, Rapid Commun. Mass Spectrom. 16 (2002) 859–864.
[13] N. Calonghi, C. Cappadone, E. Pagnotta, G. Farruggia, F. Buontempo, C. Boga, G.L. Brusa, M.A. Santucci, L. Masotti, Biochem. Biophys. Res. Commun. 314 (2004) 138–142.
[14] N. Calonghi, C. Cappadone, E. Pagnotta, C. Boga, C. Bertucci, J. Fiori, G. Tasco, R. Casadio, L. Masotti, J. Lipid Res. 46 (2005) 1596–1603.
[15] R.C. Badami, K.B. Patil, Prog. Lipid Res. 19 (1981) 119–153, and references cited therein.
[16] (a) S. El-Sharkawy, W. Yang, L. Dostal, J.P.N. Rosazza, Appl. Environ. Microbiol. 58 (1992) 2116–2122, and references cited therein; (b) W. Yang, L. Dostal, J.P.N. Rosazza, Appl. Environ. Microbiol. 59 (1993) 281–284, and references cited therein; (c) B.-N. Kim, S.-J. Yeom, D.-K. Oh, Biotechnol. Lett. 33 (2011) 993–997, references cited therein.
[17] S. Murakami, K. Satou, T. Kijima, M. Watanabe, T. Izumi, Eur. J. Lipid Sci. Technol. 113 (2011) 450–458.
[18] R.W. Miller, D. Weisleder, R. Kleiman, R.D. Plattnera, C.R. Smith Jr., Phytochemistry 16 (1977) 947–951.
[19] (a) S. Bowers, H.C. Hoch, P.H. Evans, M. Katayama, Science 232 (1986) 105–106; (b) I.D. Brodowsky, E.H. Oliw, Biochim. Biophys. Acta 1168 (1993) 68–72; (c) U. Garscha, E.H. Oliw, Anal. Biochem. 367 (2007) 238–246, and references cited therein.
[20] M.S.F. Lie Ken Jie, M. Khysar Pasha, M.S.K. Syed-Rahmatullah, Nat. Prod. Rep. 14 (1997) 163–189, and references cited therein.
[21] (a) M.B. Smith, J. March, March's Advanced Organic Chemistry: Reactions Mechanisms, and Structure, 7th ed., John Wiley & Sons, Hoboken, 2007, pp. 1799–1805; (b) E.M. Carreira, L. Kvaerno, Classics in Stereoselective Synthesis, Wiley-WCH, Weiheim, 2009 (chapter 2).
[22] (a) K. Nakamura, R. Yamanaka, T. Matsuda, T. Harada, Tetrahedron: Asymmetry 14 (2003) 2659–2681; (b) V. Fehring, R. Selke, Angew. Chem. Int. Ed. 37 (1998) 1827–1830; (c) K. Goldberg, K. Schroer, S. Lütz, A. Liese, Appl. Microbiol. Biotechnol. 76 (2007) 237–248.
[23] M. Utaka, H. Watabu, A. Takeda, J. Org. Chem. 52 (1987) 4363–4368.
[24] J. Pleiss, in: U. Bornsheuer (Ed.), Enzymes in Lipid Modification, Wiley-VCH Verlag, Weinheim, 2005, pp. 85–99.
[25] R.J. Kazlauskas, A.N.E. Weissfloch, A.T. Rappaport, L.A. Cuccia, J. Org. Chem. 56 (1991) 2656–2665.
[26] U.H. Kahlow, R.D. Schmid, J. Pleiss, Protein Sci. 10 (2001) 1942–1952.
[27] F. Haeffner, T. Norin, K. Hult, Biophys. J. 74 (1998) 1251–1262.
[28] S. Raza, L. Fransson, K. Hult, Protein Sci. 10 (2001) 329–338.
[29] (a) P. Braiuca, L.V. Knapic, C. Ferrario, L. Ebert, Gardossi, Adv. Synth. Catal. 351 (2009) 1293–1302; (b) J. Gu, J. Liu, H. Yu, J. Mol. Catal. B: Enzym. 72 (2011) 238–247.
[30] C. Boga, S. Puggioli, M. Gherpelli, G. Farruggia, E. Pagnotta, L. Masotti, P. Neyroz, Anal. Biochem. 335 (2004) 196–209.
[31] E. Wenkert, B.L. Buckwalter, A.A. Craveiro, E.L. Sanchez, S.S. Sharatchandra, J. Am. Chem. Soc. 100 (1978) 1267–1273.
[32] C. Orrenius, F. Haeffner, D. Rotticci, N. Öhrner, T. Norin, K. Hult, Biocatal. Biotransform. 16 (1998) 1–15.
[33] (a) O. Sundholm, L.T. Kanerva, ACH Models Chem. 135 (1998) 625–640; (b) X.-G. Li, M. Lähitie, M. Päiviö, L.T. Kanerva, Tetrahedron: Asymmetry 18 (2007) 1567–1573; (c) K. Lundell, T. Raijola, L.T. Kanerva, Enzyme Microb. Technol. 22 (1998) 86–93; (d) L.T. Kanerva, O. Sundholm, Acta Chem. Scand. 47 (1993) 823–825; (e) T. Ema, Curr. Org. Chem. 8 (2004) 1009–1025; (f) S. Tomić, T. Kojić-Prodić, J. Mol. Graphics Modell. 21 (2002) 241–252.
[34] M. Skjøt, L. De Maria, R. Chatterjee, A. Svendsen, S.A. Patkar, P.R. Ostergaard, J. Brask, Chembiochem 10 (2009) 520–527.
[35] C.-S. Chen, Y. Fujimoto, G. Girdaukas, C.J. Sih, J. Am. Chem. Soc. 104 (1982) 7294–7299.
[36] (a) B. Behrouzian, C.K. Savile, B. Dawson, P.H. Buist, J. Shanklin, J. Am. Chem. Soc. 124 (2002) 3277–3283; (b) P. Caruana, Bachelor Thesis, University of Bologna, Bologna (Italy), 2006.
[37] S. Bergstrŏm, G. Aulin Erdtman, B. Rolander, E. Stenhagen, S. Östling, Acta Chem. Scand. 6 (1952) 1157–1174.
[38] (a) A.P. Tullock, J. Am. Oil Chem. Soc. 41 (1964) 833–836; (b) A.P. Tullock, J. Am. Oil Chem. Soc. 43 (1966) 670–674; (c) A.P. Tullock, M. Mazurek, Lipids 11 (1976) 228–234; (d) A.P. Tullock, Org. Magn. Res. 11 (1978) 109–115.
[39] (a) R.G. Powell, C.R. Smith, C.A. Glass, I.A. Wolff, J. Org. Chem. 31 (1966) 528–533; (b) F.D. Gunstone, A.J. Sealy, J. Chem. Soc. (1963) 5772–5778; (c) T.H. Applewhite, R.G. Binder, W. Gaffield, J. Org. Chem. 32 (1967) 1173–1178.
[40] I.L.Z. Kuranova, Obshchei Khim 33 (1963) 2296–2301.
[41] (a) G. Knothe, M.O. Bagby, D. Weisleder, R.E. Peterson, J. Chem. Soc. Perkin Trans. 2 (1994) 1661–1670; (b) E.G. Perkins, J.R. Anfisen, J. Am. Oil Chem. Soc. 48 (1971) 556–562.
[42] I.L.Yu. Kuranova, D. Shenin, G.V.Z. Pigulevskii, Obshchei Khim 34 (1964) 3487–3493.
[43] A.P. Tullock, Can. J. Chem. 46 (1968) 3728–3729.